

Tobelite and NH₄⁺-rich muscovite single crystals from Ordovician Armorican sandstones (Brittany, France): Structure and crystal chemistry

ERNESTO MESTO, FERNANDO SCORDARI,* MARIA LACALAMITA, AND EMANUELA SCHINGARO

Dipartimento di Scienze della Terra e Geoambientali, Università degli Studi di Bari, via E. Orabona 4, I-70125 Bari, Italy

ABSTRACT

The crystal structures of tobelite and NH₄⁺-rich muscovite from the sedimentary rocks of the Armorican sandstones (Brittany, France) have been solved for the first time by single-crystal X-ray diffraction. The structural study was integrated by electron probe microanalyses, and X-ray photoelectron and micro-Fourier transform infrared spectroscopy. The crystals belong to the 2M₂ polytype with the following unit-cell parameters: $a = 9.024(1)$, $b = 5.2055(6)$, $c = 20.825(3)$ Å, and $\beta = 99.995(8)^\circ$ for tobelite and $a = 9.027(1)$, $b = 5.1999(5)$, $c = 20.616(3)$ Å, and $\beta = 100.113(8)^\circ$ for NH₄⁺-rich muscovite. Structure refinements in the space group C2/c converged at $R_1 = 8.01\%$, $wR_2 = 8.84\%$ and $R_1 = 5.59\%$, $wR_2 = 5.63\%$ for tobelite and NH₄⁺-rich muscovite, respectively.

X-ray photoelectron spectroscopy revealed nitrogen environments associated either with inorganic (B.E. 401.31 eV) or organic (B.E. 398.67 eV) compounds. Infrared spectra showed, in the OH⁻-stretching region (3700–3575 cm⁻¹), two prominent bands, centered at ~3629 and ~3646 cm⁻¹, and two shoulders at ~3664 and ~3615 cm⁻¹ that were assigned to Al³⁺Al³⁺□-OH⁻ arrangements having OH⁻ groups affected by different local configurations. In addition, a series of overlapping bands from about 3500 to 2700 cm⁻¹ characteristic of the NH₄⁺-stretching vibrations, a main band at ~1430 and a shoulder at ~1460 cm⁻¹ that were associated to the NH₄⁺-bending vibration (ν_4) were also present.

The ammonium concentration was semi-quantitatively estimated in both crystals from the absorbance of the OH⁻-stretching and NH₄⁺-bending vibrations in the infrared spectra. An additional estimate was obtained for the NH₄⁺-rich muscovite by considering the normalized peak area between K2p_{3/2} and N1s in the X-ray photoelectron spectrum. The obtained values are in agreement with those derived from the interlayer spacing in the simulated X-ray powder diffraction spectra.

The results of this integrated approach converged to (K_{0.18}Na_{0.01}NH₄^{0.62})_{Σ=0.81}(Al_{1.98}Fe_{0.02}²⁺)_{Σ=2.00}(Si_{3.19}Al_{0.81})_{Σ=4.00}O_{10.00}OH_{2.00} for tobelite and to (K_{0.46}Na_{0.03}Ba_{0.01}NH₄^{0.36})_{Σ=0.86}(Al_{1.98}Mg_{0.01}Fe_{0.01}V_{0.01}³⁺)_{Σ=2.01}(Si_{3.13}Al_{0.87})_{Σ=4.00}O_{10.00}F_{0.08}OH_{1.92} for NH₄⁺-rich muscovite.

Keywords: Tobelite, NH₄⁺-rich muscovite, 2M₂ polytype, crystal chemistry, NH₄⁺ estimation, SCXRD, XPS, micro-FTIR

INTRODUCTION

Tobelite is a dioctahedral mica with ideal composition (NH₄)Al₂(Si₃Al)O₁₀(OH)₂. Tobelite was first found by Higashi (1982) in the Ohgidani pottery stone deposit at Tobe (Japan) as the product of a hydrothermally altered biotite andesite dike. This mica exhibited high NH₄⁺ concentration (0.53 gpfu, groups per formula unit). X-ray powder diffraction indicated that it belongs to the 1M polytype, space group C2/m with lattice parameters $a = 5.219(4)$, $b = 8.986(3)$, $c = 10.447(2)$ Å, and $\beta = 101.31(1)^\circ$ (Higashi 1982). Several studies since then have been devoted to natural ammonium-bearing micas or to their synthetic counterparts. Natural crystals having NH₄⁺ contents up to 0.75 gpfu (Ruiz Cruz and Sanz de Galdeano 2008) have been reported to date and several authors hypothesized a complete solid solution between tobelite and muscovite (Juster et al. 1987; Wilson et al. 1992; Drits et al. 1997; Liang et al. 1997). However, Nieto (2002) showed that a miscibility gap between muscovite and tobelite

may occur at temperatures below 300 °C.

Ammonium-rich micas are generally found in very low to low grade metamorphic rocks (e.g. Honna and Itihara 1981; Itihara and Suwa 1985; Duit et al. 1986; Visser 1992; Boyd and Philippot 1998; Mingram and Brauer 2001). Only recently, a NH₄⁺-rich white mica formed at higher temperature (>400 °C) was discovered in polymetamorphic schists from the Internal Zone of the Betic Cordillera, Spain (Ruiz Cruz and Sanz de Galdeano 2008). The same authors later discovered and characterized the trioctahedral analog of tobelite, suhailite, with composition [Ca_{0.04}Na_{0.07}K_{0.35}(NH₄)_{0.55}]_{Σ=1.01}(Al_{0.42}Ti_{0.22}Fe_{1.33}Mn_{0.01}Mg_{0.71})_{Σ=2.69}(Si_{2.67}Al_{1.33})_{Σ=4.00}O₁₀(OH)₂ (Ruiz Cruz and Sanz de Galdeano 2009).

Most of the studies reported to date on ammonium-rich micas have dealt with the mechanisms involved in the “tobelitization processes” during diagenesis and oil formation (see Dainyak et al. 2006 and references therein). Indeed, the importance of the ammonium-rich micas is that they form in organic-rich source rocks and under conditions of unusually N-enriched hydrother-

* E-mail: f.scordari@geomin.uniba.it

mal fluid circulation. In addition, their occurrence has thermo-barometric implications (Ruiz Cruz 2011 and references therein). Studies on synthetic ammonium-bearing micas have concerned mainly the various synthesis procedures and the characterization of very small single crystals or powder samples (see Pöter et al. 2007 and references therein).

To date, the structural characterization of ammonium-bearing micas has been accomplished primarily by means of X-ray powder diffraction (see, for instance, Higashi 1982, 2000; Juster et al. 1987; Wilson et al. 1992; Nieto 2002; Pöter et al. 2007; Ruiz Cruz 2011; Ruiz Cruz and Sanz de Galdeano 2008, 2010), accompanied by Rietveld based analyses in some cases (Harlov et al. 2001; Pöter et al. 2007). Specifically, Rietveld analyses allow: (1) identification and quantification of the mica polytypes as well determination of the cell parameters (Harlov et al. 2001; Pöter et al. 2007); and (2) quantification of mineral phase mixtures (Harlov et al. 2001; Pöter et al. 2007; Ruiz Cruz 2011). Atomic coordinates and other crystallographic parameters were not refined in any of the aforementioned studies. Tobelite was found to belong to the *1M* polytype (Higashi 1982; Hovis et al. 2004) or to be a mixture of *1M*, *2M*₁, *2M*₂, *3T*, and *2Or* polytypes (Harlov et al. 2001; Pöter et al. 2007). The ammonium content was quantified by means of electron microprobe (Higashi 1982, 2000; Ruiz Cruz 2011) and elemental analysis (Schroeder and Ingall 1994; Schroeder and McLain 1998; Ruiz Cruz 2011; Ruiz Cruz and Sanz de Galdeano 2008, 2010); the ammonium content was estimated by means of X-ray powder diffraction and infrared spectroscopic methods (Higashi 2000; Nieto 2002; Pironon et al. 2003; Pöter et al. 2007; Ruiz Cruz 2011; Ruiz Cruz and Sanz de Galdeano 2008).

In the present work, for the first time, the tobelite structure was refined from single-crystal X-ray diffraction (SCXRD) data. The study was accompanied by electron probe microanalysis (EPMA), X-ray photoelectron spectroscopy (XPS), and micro-Fourier transform infrared spectroscopy (micro-FTIR).

EXPERIMENTAL METHODS

Sample description

The studied crystals are from the sandstones of the Ordovician Armorican Massif (Brittany, France). The rocks were metamorphosed and hydrothermally altered at low temperature under very reducing conditions in the presence of abundant organic matter. The mica is associated with chlorite (chamosite), dolomite, quartz, tourmaline, chalcopyrite, galena, sulfosalts (boulangerite, bournonite, tetrahedrite), and electrum. The temperature of mica formation is estimated to be ~275 °C (J.-L. Robert, personal communication). Figure 1 shows that the tobelite protruded from the host rock making it possible to separate and select single crystals by hand-picking. In particular, two crystals were investigated by EPMA, SCXRD, and spectroscopic methods, and are labeled Musc_4 and Tob_7.

Electron probe microanalysis

Chemical compositions of the same single crystals used for X-ray diffraction analysis were determined with a Cameca SX-50 electron microprobe after embedding in epoxy resin and polishing. Operating conditions were: 15 kV accelerating voltage, 15 nA specimen beam current, and 10 μm beam diameter. The analyses were carried out in full wavelength-dispersive spectrometry (WDS) mode. The following standards were used: wollastonite (Si-Ca), olivine (Mg), magnetite (Fe), corundum (Al), orthoclase (K), rutile (Ti), jadeite (Na), barite (Ba), vanadinite (V), phlogopite (F), sylvite (Cl), metallic Mn, Ni, and chromium. Conversion from X-ray counts to oxide wt% was accomplished using the Pouchou and Pichoir (1985) (PAP) matrix correction software package.

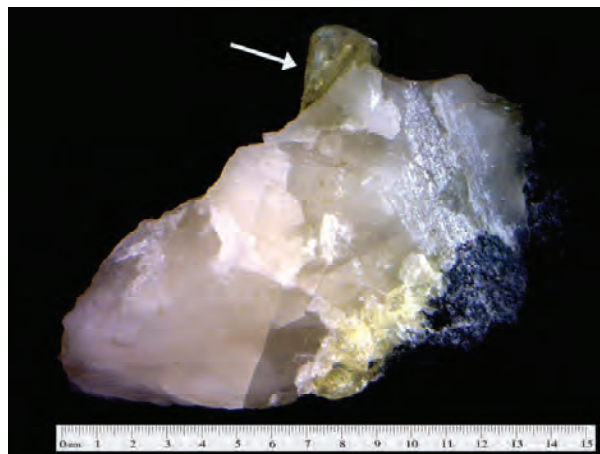


FIGURE 1. Optical picture of the study tobelite specimen (indicated by the arrow) and its host rock. (Color online.)

X-ray photoelectron spectroscopy

X-ray photoelectron spectroscopy was done using a VG Theta Probe spectrometer equipped with a monochromatized AlK α source and a flood gun for sample charge compensation. Survey spectra and high-resolution spectra (for K2p, N1s, and C1s regions) were recorded in fixed analyzer transmission mode, with a pass energy of 200 and 30 eV, respectively. Binding energies were calibrated with respect to the adventitious C1s (284.5 eV) signal.

Single-crystal X-ray diffraction

Preliminary X-ray diffraction analysis suggested that the micas under investigation were characterized by a very bad diffraction behavior. Out of 40 single crystals tested, only Musc_4 and Tob_7 proved to be suitable for X-ray data collection. X-ray diffraction intensity data were measured with a Bruker AXS X8 APEXII diffractometer equipped with a four-circle Kappa goniometer and a charge coupled device (CCD) detector. The X-ray data were collected at room temperature using MoK α radiation, a combination of ϕ - ω scans, and long exposure times (from 30 to 45 s/frame for Musc_4, and from 180 to 540 s/frame for Tob_7). Cell determination and data reduction were performed with the SAINT (Siemens 2004) and SADABS programs (Sheldrick 2004). The structure was solved from scratch by direct methods and successive difference Fourier synthesis using the SIR2002 program (Burla et al. 2003). The structural refinements were carried out in space group *C2/c* using CRYSTALS (Betteridge et al. 2003).

Fourier transform infrared spectroscopy

Transmission micro-FTIR measurements were performed in the spectral range 4000–650 cm⁻¹ with a nominal resolution of 4 cm⁻¹ using a Nicolet Avatar FTIR spectrometer equipped with a continuum microscope, mercury cadmium telluride (MCT) nitrogen-cooled detector, and KBr beamsplitter. The crystals, mounted on glass capillaries, were analyzed with the infrared beam normal to the cleavage plane. The final spectra were averaged over 128 scans. The background correction was made using a linear function. Peak fitting was accomplished with a Gaussian function using the program PeakFit by Jandel Scientific.

RESULTS

Chemical composition

The average chemical compositions of the micas are shown in Table 1 (4 and 6 point analyses for Musc_4 and Tob_7, respectively). The main differences between Musc_4 and Tob_7 crystals are related to the concentrations of K₂O [5.66(4) vs. 2.2(1) wt%], BaO [0.28(3) vs. 0.05(4) wt%], and F [0.41(2) vs. 0.01(3) wt%], respectively.

Structure determination and refinement

Crystal data and experimental details and figures of merit of the structure refinement are summarized in Table 2. The structural solution showed the samples to belong to the 2M₂ polytype. Fully isotropic refinements resulted in $R_1 = 7.6\%$, $wR_2 = 8.0\%$ and $R_1 = 10.5\%$, $wR_2 = 11.5\%$ for Musc_4 and Tob_7, respectively. Because the crystals analyzed have inherently low X-ray scattering power, the N/p (number of reflections over the refined parameters) ratio did not allow us to perform fully anisotropic refinements. Partially anisotropic refinements (only for non-oxygen atoms) converged to $R_1 = 6.9\%$, $wR_2 = 7.4\%$ and $R_1 = 8.0\%$, $wR_2 = 8.8\%$ for Musc_4 and Tob_7, respectively.

The $h0l$ and $0kl$ calculated precessions images (reported in Fig. 2 are those relevant to sample Musc_4) indicate that the crystal quality is poor (presence of broadened peaks and of streaks along the c^* direction). Thus, the samples are affected by stacking disorder, which is more pronounced for Tob_7 (with greater NH₄⁺ content) than for the Musc_4 crystal. Another kind of disorder was detected by analysis of difference Fourier maps of both crystals. It shows up as systematic residual density of about $2 \text{ e}^-/\text{\AA}^3$ around the M2, T1, and T2 sites, distributed in

the structure as pairs parallel to the [001] direction and symmetrically located with respect to the atoms of the structure. The additional TOT sheets were introduced into the structure refinement for Musc_4, which could undergo a rigid $\pm z$ translation across the interlayer site. This model further decreased the R_1 index to 5.59% and the wR_2 index to 5.63%, and the residual electron density became featureless. It is interesting to note that the refined translation of the disordered TOT layers leads to a shrinkage of the interlayer thickness of $\sim 0.65 \text{ \AA}$. The relatively lower quality (N/p ratio) of the Tob_7 data set did not allow us to use the same disorder modeling.

Final atomic coordinates, site occupancies, and atomic displacement parameters are given in Table 3, as well as the parameters of the $\pm z$ shifted layers for the Musc_4 crystal. Atom labeling is after Zhoukhlistov et al. (1973). Selected bond distances and mean

TABLE 1. Chemical composition (EPMA, wt%) of the studied micas

	Musc_4	Tob_7
SiO ₂	49.4(1)	50.7(7)
Al ₂ O ₃	38.3(1)	37.6(6)
MgO	0.07(3)	0.04(2)
FeO	0.24(2)	0.37(4)
TiO ₂	0.02(3)	0.08(4)
V ₂ O ₅	0.12(1)	0.02(3)
MnO	0.01(2)	0.02(3)
NiO	n.d.	0.01(2)
Cr ₂ O ₃	n.d.	0.01(2)
K ₂ O	5.66(4)	2.2(1)
Na ₂ O	0.23(2)	0.07(2)
BaO	0.28(3)	0.05(4)
CaO	0.04(1)	0.04(4)
F	0.41(2)	0.01(3)
Cl	0.03(1)	0.02(1)
Total	94.8(1)	91.2(9)

Note: n.d. = not determined.

TABLE 2. Summary data about collection and refinement of the studied micas

	Musc_4	Tob_7
Crystal size (mm ³)	0.20 × 0.15 × 0.01	0.18 × 0.12 × 0.01
Space group	C2/c	C2/c
<i>a</i> (Å)	9.027(1)	9.024(1)
<i>b</i> (Å)	5.1999(5)	5.2055(6)
<i>c</i> (Å)	20.616(3)	20.825(3)
β (°)	100.113(8)	99.995(8)
Cell volume (Å ³)	952.6(2)	963.4(2)
<i>Z</i>	4	4
θ range for data collection	4 to 40°	4 to 40°
Reflections collected	3569	5407
Reflections unique	940	998
R_{merging} (R_{int}) (%)	5.30	8.18
Reflections used [$I > 3\sigma(I)$]	540	427
No. of refined parameters	73	63
Goof*	1.151	1.16
R_1 † [on F] (%)	5.59	8.01
wR_2 ‡ [on F^2] (%)	5.63	8.84
$\Delta\rho_{\text{min}}/\Delta\rho_{\text{max}}$ (e ⁻ /Å ³)	-0.77/0.62	-1.13/1.71

* Goodness-of-fit = $\{\sum[w(F_o - F_c)^2]/(N - p)\}^{1/2}$, where N and p are the number of reflections and parameters, respectively.

† $R_1 = \sum|F_o| - |F_c|/\sum|F_o|$.

‡ $wR_2 = \{\sum[w(F_o^2 - F_c^2)^2]/\sum[w(F_o^2)^2]\}^{1/2}$; w = Chebyshev optimized weights.

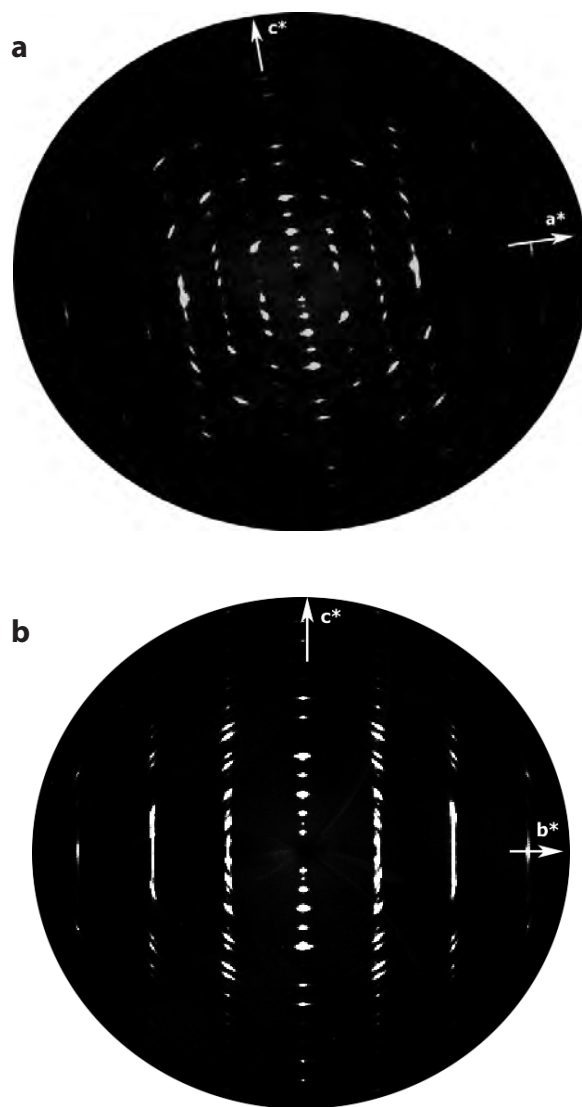


FIGURE 2. Musc_4 crystal: (a) $h0l$ and (b) $0kl$ simulated precessions.

TABLE 3. Crystallographic coordinates, occupancies, equivalent isotropic (\AA^2), and anisotropic displacement parameters of the studied micas

Site	Atom	x	y	z	Occupancy	$U_{\text{iso/equiv}}$	U_{11}	U_{22}	U_{33}	U_{23}	U_{13}	U_{12}
Sample Musc_4												
K	K ⁺	0	0.1042(9)	¼	0.465(8)	0.029	0.027(2)	0.024(2)	0.035(3)	0	0.0048(18)	0
	N	0	0.1042(9)	¼	0.50(2)	0.029	0.027(2)	0.024(2)	0.035(3)	0	0.0048(18)	0
M2	Al ³⁺	0.0830(2)	0.2500(4)	0.0001(1)	0.929(8)	0.0111	0.013(1)	0.008(1)	0.013(1)	0.0020(9)	0.0029(8)	0.0007(9)
T1	Si ⁴⁺	0.1232(2)	0.5864(4)	0.1333(1)	0.940(8)	0.0128	0.0117(9)	0.011(1)	0.016(1)	0.0007(8)	0.0036(8)	0.0012(8)
T2	Si ⁴⁺	0.2948(2)	0.1047(4)	0.13315(9)	0.938(8)	0.0144	0.014(1)	0.011(1)	0.019(1)	-0.0011(9)	0.0053(9)	-0.0020(8)
O1	O ²⁻	0.0785(6)	0.558(1)	0.0528(2)	0.940(8)	0.015(1)	-	-	-	-	-	-
O2	O ²⁻	0.2704(6)	0.137(1)	0.0528(2)	0.942(8)	0.016(1)	-	-	-	-	-	-
O3	O ²⁻	0.1964(6)	0.318(1)	0.1659(2)	0.932(8)	0.017(1)	-	-	-	-	-	-
O4	O ²⁻	0.4722(6)	0.148(1)	0.1652(3)	0.933(8)	0.020(1)	-	-	-	-	-	-
O5	O ²⁻	0.2491(6)	0.813(1)	0.1539(3)	0.941(8)	0.022(1)	-	-	-	-	-	-
O6	OH	0.9567(5)	0.0597(9)	0.0490(2)	0.93(1)	0.012(1)	-	-	-	-	-	-
Shifted layer												
M2 _(-z)	Al ³⁺	0.078(2)	0.261(2)	-0.032(1)	0.032(2)	0.0111	0.013(1)	0.008(1)	0.013(1)	0.0020(9)	0.0029(8)	0.0007(9)
T1 _(-z)	Si ⁴⁺	0.118(2)	0.592(2)	0.101(1)	0.032(2)	0.0128	0.0117(9)	0.011(1)	0.016(1)	0.0007(8)	0.0036(8)	0.0012(8)
T2 _(-z)	Si ⁴⁺	0.290(2)	0.116(2)	0.101(1)	0.032(2)	0.0144	0.014(1)	0.011(1)	0.019(1)	-0.0011(9)	0.0053(9)	-0.0020(8)
O1 _(-z)	O ²⁻	0.073(2)	0.568(2)	0.021(1)	0.032(2)	0.015(1)	-	-	-	-	-	-
O2 _(-z)	O ²⁻	0.263(2)	0.148(2)	0.021(1)	0.032(2)	0.016(1)	-	-	-	-	-	-
O3 _(-z)	O ²⁻	0.193(2)	0.328(2)	0.134(1)	0.032(2)	0.017(1)	-	-	-	-	-	-
O4 _(-z)	O ²⁻	0.467(2)	0.158(2)	0.133(1)	0.032(2)	0.020(1)	-	-	-	-	-	-
O5 _(-z)	O ²⁻	0.243(2)	0.821(2)	0.122(1)	0.032(2)	0.022(1)	-	-	-	-	-	-
O6 _(-z)	OH	0.949(2)	0.071(2)	0.017(1)	0.032(2)	0.012(1)	-	-	-	-	-	-
M2 _(+z)	Al ³⁺	0.078(2)	0.261(2)	0.032(1)	0.032(2)	0.0111	0.013(1)	0.008(1)	0.013(1)	0.0020(9)	0.0029(8)	0.0007(9)
T1 _(+z)	Si ⁴⁺	0.118(2)	0.592(2)	0.165(1)	0.032(2)	0.0128	0.0117(9)	0.011(1)	0.016(1)	0.0007(8)	0.0036(8)	0.0012(8)
T2 _(+z)	Si ⁴⁺	0.290(2)	0.116(2)	0.165(1)	0.032(2)	0.0144	0.014(1)	0.011(1)	0.019(1)	-0.0011(9)	0.0053(9)	-0.0020(8)
O1 _(+z)	O ²⁻	0.073(2)	0.568(2)	0.085(1)	0.032(2)	0.015(1)	-	-	-	-	-	-
O2 _(+z)	O ²⁻	0.263(2)	0.148(2)	0.085(1)	0.032(2)	0.016(1)	-	-	-	-	-	-
O3 _(+z)	O ²⁻	0.193(2)	0.328(2)	0.198(1)	0.032(2)	0.017(1)	-	-	-	-	-	-
O4 _(+z)	O ²⁻	0.467(2)	0.158(2)	0.197(1)	0.032(2)	0.020(1)	-	-	-	-	-	-
O5 _(+z)	O ²⁻	0.243(2)	0.821(2)	0.186(1)	0.032(2)	0.022(1)	-	-	-	-	-	-
O6 _(+z)	OH	0.949(2)	0.071(2)	0.081(1)	0.032(2)	0.012(1)	-	-	-	-	-	-
Sample Tob_7												
K	K ⁺	0	0.114(3)	¼	0.201(1)	0.0257	0.0299(7)	0.019(6)	0.026(7)	0	-0.001(5)	0
	N	0	0.114(3)	¼	0.780(1)	0.0257	0.0299(7)	0.019(6)	0.026(7)	0	-0.001(5)	0
M2	Al ³⁺	0.0822(5)	0.2492(9)	-0.0002(3)	0.999(1)	0.0109	0.0087(9)	0.004(2)	0.020(2)	0.003(2)	0.004(2)	0.001(2)
T1	Si ⁴⁺	0.1216(4)	0.5852(7)	0.1316(2)	1.005(1)	0.0118	0.0048(8)	0.005(2)	0.027(3)	0.001(2)	0.007(2)	-0.001(2)
T2	Si ⁴⁺	0.2938(4)	0.1048(7)	0.1318(2)	1.000(1)	0.0129	0.0085(8)	0.001(2)	0.030(3)	-0.001(2)	0.005(2)	0.001(2)
O1	O ²⁻	0.077(1)	0.558(2)	0.0526(5)	1.000	0.0124(9)	-	-	-	-	-	-
O2	O ²⁻	0.270(1)	0.136(2)	0.0528(5)	1.000	0.0164(9)	-	-	-	-	-	-
O3	O ²⁻	0.195(1)	0.320(2)	0.1640(5)	1.000	0.0207(9)	-	-	-	-	-	-
O4	O ²⁻	0.470(1)	0.148(2)	0.1633(5)	1.000	0.0169(9)	-	-	-	-	-	-
O5	O ²⁻	0.248(1)	0.814(2)	0.1531(5)	1.000	0.0141(9)	-	-	-	-	-	-
O6	OH	0.956(1)	0.057(2)	0.0480(5)	1.000	0.0153(9)	-	-	-	-	-	-

Notes: The atomic coordinates for the layers shifted of $-z$ and $+z$ with respect to the interlayer are reported (see text for details).

atomic numbers of cation sites as determined by structure refinement (X-ref) and electron probe microanalyses, and distortional parameters are reported in Tables 4 and 5, respectively. CIF files are available on deposit.¹

The cell parameters of the studied crystals (Table 2) are in the range of variability already reported in the literature for $2M_2$ ammonium-rich muscovite: $a = 9.023(2)$ – $9.032(3)$, $b = 5.191(3)$ – $5.207(2)$, $c = 20.460(7)$ – $21.011(1)$ Å, and $\beta = 99.71(5)$ – $100.04(4)^\circ$ (Pöter et al. 2007). Note that only two single-crystal structure refinements of $2M_2$ dioctahedral micas have been documented to date: one is relevant to a phengite- $2M_2$ structure determined by electron diffraction (Zhoukhlistov et al. 1973), and the other is a determination of the nanpingite- $2M_2$ structure (Ni and Hughes 1996). A comparison of the data of this study and literature samples is discussed below.

¹ Deposit item AM-12-054, CIF. Deposit items are available two ways: For a paper copy contact the Business Office of the Mineralogical Society of America (see inside front cover of recent issue) for price information. For an electronic copy visit the MSA web site at <http://www.minsocam.org>, go to the *American Mineralogist* Contents, find the table of contents for the specific volume/issue wanted, and then click on the deposit link there.

Hydrogen and nitrogen speciation

The results of the X-ray photoelectron spectroscopy investigation are reported in Figures 3 and 4. Figure 3 shows the survey scan of the Musc_4 crystal. The analysis was not performed on the Tob_7 crystal because it was lost after FTIR and electron microprobe analysis. All of the expected peaks relevant to the fundamental mica constituents are present, specifically Si2p (B.E. 108.98 eV), N1s (B.E. 399.99 eV), K2p_{3/2} (B.E. 287.55 eV), O1s (B.E. 531.41 eV), and Al2p (B.E. 73.73 eV). The narrow scan measured on the N1s region (Fig. 4) resulted in asymmetrical peak, which can be fitted with two components corresponding to: (1) NH₄⁺ in an inorganic component (B.E. 401.31 eV); and (2) nitrogen in organic compounds (-NH₂, B.E. 398.67 eV). By considering the normalized peak area between K2p_{3/2} and N1s (inorganic component), the approximate K/N ratio in the Musc_4 sample is ~1.

Results of FTIR investigation on the Musc_4 sample are reported in Figure 5. Musc_4 and Tob_7 samples yielded similar spectra, such that only the spectrum of the Musc_4 crystal in the range 3800–1300 cm⁻¹ is illustrated in Figure 5a. The results of

the fits for the OH⁻- and NH₄⁺-stretching regions are shown in Figures 5b and 5c, respectively. Band positions and their assignments are summarized in Table 6.

The OH⁻-stretching region (3700–3575 cm⁻¹) of the studied crystal consists of two prominent bands (see Fig. 5b and Table 6),

TABLE 4. Selected bond distances (Å), mean atomic numbers (electrons, e⁻) of cation sites as determined by structure refinement (X-ref), and chemical determinations (EPMA) of the studied micas

	Musc_4	Tob_7
T1-O1	1.643(5)	1.63(1)
T1-O3	1.638(5)	1.63(1)
T1-O4	1.646(5)	1.65(1)
T1-O5	1.641(6)	1.66(1)
<T1-O>	1.642	1.64
T2-O2	1.640(5)	1.63(1)
T2-O3	1.638(5)	1.64(1)
T2-O4	1.636(6)	1.63(1)
T2-O5	1.648(6)	1.65(1)
<T2-O>	1.641	1.64
<T-O>	1.642	1.64
M2-O1	1.937(6)	1.93(1)
M2-O1'	1.940(6)	1.95(1)
M2-O2	1.935(6)	1.95(1)
M2-O2'	1.948(5)	1.96(1)
M2-O6	1.902(5)	1.88(1)
M2-O6'	1.924(5)	1.92(1)
<M2-O>	1.931	1.93
K-O3 (x2)	2.910(5)	2.92(1)
K-O3' (x2)	3.327(6)	3.38(1)
K-O4 (x2)	2.930(6)	3.01(2)
K-O4' (x2)	3.313(6)	3.30(2)
K-O5 (x2)	2.942(6)	2.95(1)
K-O5' (x2)	3.583(6)	3.62(1)
<K-O> _{inner}	2.927	2.96
<K-O> _{outer}	3.408	3.43
<K-O>	3.168	3.20
M2 e ⁻ _{X-ref}	12.91	12.99
M2 e ⁻ _{EPMA}	13.18	13.13
K e ⁻ _{X-ref}	12.34	9.28
K e ⁻ _{EPMA}	13.23	9.73
T e ⁻ _{X-ref}	14.04	14.04
T e ⁻ _{EPMA}	13.78	13.80
Σ ⁺	22.01	21.98
Σ ⁻	22.00	22.00

Notes: Average error for mean atomic numbers is ±0.5 e⁻. Σ⁺ and Σ⁻ are sum of positive and negative charges, respectively.

centered at ~3629 (band III) and ~3646 cm⁻¹ (band II), and of two shoulders at ~3663 (band I) and ~3614 cm⁻¹ (band IV). These results are in agreement with previous studies on tobelite samples and ammonium-rich muscovite grains, all of which reported the OH⁻ absorption peak at about 3630 cm⁻¹ (Higashi 1982; Harlov et al. 2001; Mookherjee et al. 2002; Nieto 2002; Pironon et al. 2003; Pöter et al. 2007). In particular, Harlov et al. (2001) and, more recently, Pöter et al. (2007) ascribed this signal to Al³⁺Al³⁺□-OH⁻ arrangements whose OH⁻ groups are affected by different tetrahedral configurations. Figure 5b displays a series of overlapping bands from 3500 to 2700 cm⁻¹, which are characteristic of normal modes of vibration of the ammonium ion (NH₄⁺) (see bands V to IX in Table 6). Specifically, the bands are associated with the NH₄⁺-stretching vibration ν₁, ν₃, the combination mode ν₂+ν₄, and the overtones 2ν₂ and 2ν₄ (Higashi 1982; Harlov et al. 2001; Mookherjee et al. 2002; Nieto 2002; Pironon et al. 2003). Finally, the main band at ~1430 cm⁻¹ and the shoulder at ~1460 cm⁻¹ are due to the NH₄⁺-bending vibration ν₄, confirming the assignment of the peaks in the NH₄⁺-stretching vibration region.

Estimate of the NH₄⁺ concentration

The ammonium content of the studied crystals was semi-quantitatively estimated from the FTIR spectra using the procedure devised by Higashi (2000). This procedure takes into account the absorbance of the OH⁻-stretching and NH₄⁺-bending vibrations. The values obtained for (NH₄)₂O were 2.63 and 4.04 wt% (0.38 and 0.59 gpfu) for Musc_4 and Tob_7, respectively. The same measurements were also performed on other crystals from the same rock sample. The (NH₄)₂O content was found to be in the range of 2.44–4.53 wt% (0.36–0.66 gpfu), indicating that the values determined for the Musc_4 and Tob_7 crystals describe the variability of the (NH₄)₂O of tobelite in the host rock. Following Higashi (2000), an independent estimate of the ammonium content for the samples was obtained from the *d*₀₀₈ and *d*₀₁₀ spacing of the simulated X-ray powder diffraction spectra. The values NH₄⁺/(K+NH₄⁺+Na+Ba) = 0.41 for Musc_4 and 0.71 for Tob_7 crystals recalculate back to 2.40 and 4.50 (NH₄)₂O wt% (0.35 and 0.65 gpfu), respectively. Similar results

TABLE 5. Selected distortional parameters from the structure refinements of the studied micas and of the literature dioctahedral 2M₂ and 2M₁ micas

	Musc_4	Tob_7	2M ₂ -phengite*	2M ₂ -nanpingite†	2M ₁ -paragonite‡	2M ₁ -muscovite§	2M ₁ -muscovite
t _{tet} (Å)	2.221	2.205	2.208	2.216	2.216	2.220	2.226
t _{oct} (Å)	2.092	2.095	2.135	2.079	2.077	2.088	2.090
t _{int} (Å)	3.577	3.678	3.409	3.989	3.053	3.379	3.408
Volume _{T1} (Å ³)	2.269	2.842	2.164	2.233	2.312	2.256	2.275
Volume _{T2} (Å ³)	2.266	2.665	2.309	2.229	2.314	2.268	2.279
τ _{T1} (°)	108.3	105.9	107.1	107.5	110.3	111.1	111.0
τ _{T2} (°)	108.1	109.2	107.2	107.4	110.3	111.0	111.0
α (°)	10.92	11.72	11.21	5.74	16.29	11.30	11.39
Δz (Å)	0.244	0.224	0.234	0.215	0.231	0.224	0.230
ψ _{M1} (°)	62.30	62.32	60.90	62.40	62.12	62.26	62.29
ψ _{M2} (°)	57.20	57.16	56.94	57.57	57.02	57.12	57.13
Volume _{M1} (Å ³)	14.363	14.442	13.590	14.230	13.851	14.246	14.315
Volume _{M2} (Å ³)	9.380	9.389	9.780	9.514	9.040	9.253	9.278

Notes: t_{tet} = tetrahedral sheet thickness calculated from z coordinates of basal and apical O atoms; t_{oct} = octahedral sheet thickness (Toraya 1981); t_{int} = calculated from the z coordinates of basal O atoms; τ = tetrahedral flattening angle; α: tetrahedral rotation angle (Hazen and Burnham 1973); Δz = departure from coplanarity of the basal O atoms (Güven 1971); ψ = octahedral flattening angles (Donnay et al. 1964a, 1964b).

* Zhoukhlistov et al. (1973).

† Ni and Hughes (1996).

‡ Lin and Bailey (1984).

§ Sample RA1 from Brigatti et al. (1998).

|| Sample C3-29b from Brigatti et al. (1998).

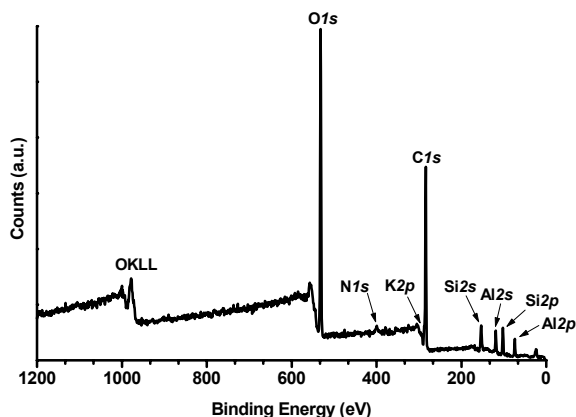


FIGURE 3. Musc_4 crystal: XPS wide scan.

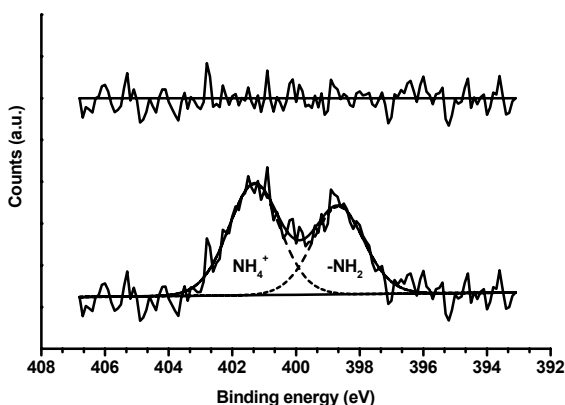
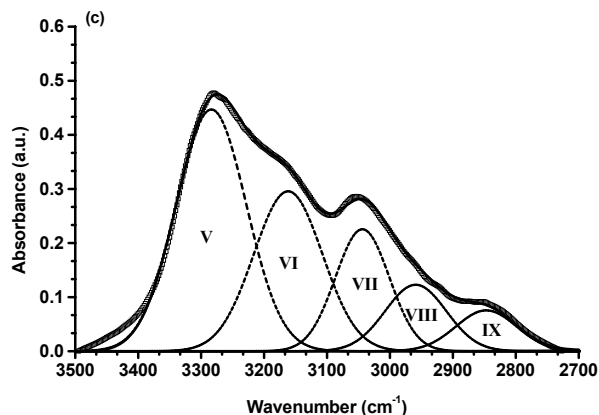
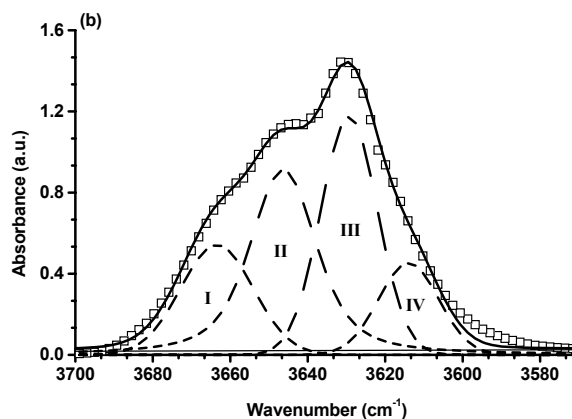
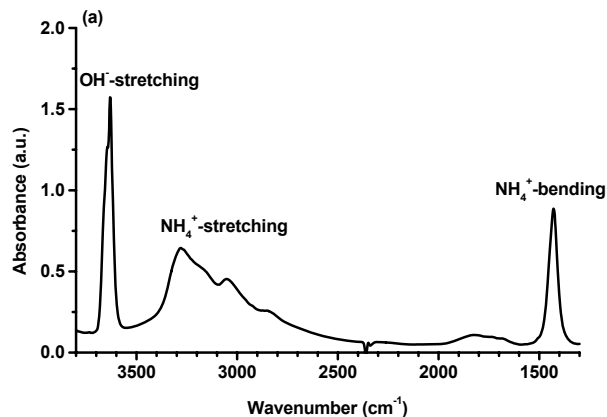


FIGURE 4. Musc_4 crystal: XPS narrow scan in the N1s region.

were obtained by applying the procedure proposed in Drits et al. (1997). Note that the high (NH₄)₂O value estimated for the Tob_7 crystal approaches that of ideal tobelite (6.90 wt%, 1 gpfu). Finally, Pöter et al. (2007) showed that the *a*, *b*, and *c* lattice parameters are a linear function of the chemical composition in the tobelite-muscovite series (see their Fig. 9). The NH₄⁺-estimates and the experimental lattice constants of Musc_4 and Tob_7 crystals follow the trend found by Pöter et al. (2007) for the case of their 2M₂ polytype.

DISCUSSION

The structural formulas [based on 12 (O, OH, F, Cl), the estimates of NH₄⁺ from FTIR and X-ray diffraction data, and charge-balance requirements] are shown in Table 7. The K/N ratio in the Musc_4 sample is in agreement with the approximate value (~1) estimated from the XPS spectrum (see Table 7 and the Hydrogen and nitrogen speciation section). Note that, from a classification viewpoint (Rieder et al. 1998), only the Tob_7 crystal can be termed “tobelite,” with NH₄⁺ (gpfu) > K⁺ (apfu). The Musc_4 crystals, with NH₄⁺ (gpfu) < K⁺ (apfu), is defined an ammonium-rich muscovite. The chemical variations of the tobelite and NH₄⁺-rich muscovite crystals studied can be explained by the following mechanisms: ^{XII}K⁺ ↔ ^{XII}NH₄⁺; ^{VI}M³⁺+^{IV}Al³⁺ ↔ ^{VI}M²⁺+^{IV}Si⁴⁺ (where ^{VI}M³⁺ = Al³⁺, Fe³⁺, V³⁺, and ^{VI}M²⁺ = Mg²⁺).

FIGURE 5. Musc_4 crystal: (a) FTIR spectrum in the region 3800–1375 (cm⁻¹); (b) Results of fitting of the OH⁻-stretching vibration; (c) Results of fitting of the NH₄⁺-stretching vibration.

The structural formulas of other natural ammonium micas and tobelite grains from different localities (Higashi 1982; Wilson et al. 1992; Ruiz Cruz 2011; Ruiz Cruz and Sanz de Galdeano 2008) as well as of synthetic samples (Harlov et al. 2001; Pöter et al. 2007) are reported in Table 7. A comparison with literature samples is also shown in Figure 6, in the form of NH₄⁺ vs. ^{XII}R-NH₄⁺ (where R represents the sum of the non-NH₄⁺

TABLE 6. FTIR spectra: band position (cm⁻¹) and assignment

Band	Musc_4	Tob_7	Band assignment	Literature data
I	3663	3664	Al ³⁺ Al ³⁺ □-OH ⁻	3665† 3660#
II	3646	3645	Al ³⁺ Al ³⁺ □-OH ⁻	3645#
III	3629	3630	Al ³⁺ Al ³⁺ □-OH ⁻	3635† 3640‡ 3631§ 3633 3632#
IV	3614	3615	Al ³⁺ Al ³⁺ □-OH ⁻	~3610#
V	3284	3277	v ₃ NH ₄ ⁺	3310–3280* 3455–3300† 3423‡ 3305§ 3295
VI	3162	3155	2v ₂ NH ₄ ⁺	3160–3140* 3175† 3129‡ 3174§
VII	3044	3044	v ₂ + v ₄ NH ₄ ⁺	3040* 3035† 3052§ 3040
VIII	2959	2959	v ₁ NH ₄ ⁺	2860* 2850§
IX	2847	2848	2v ₄ NH ₄ ⁺	2830* 2825† 2855‡ 2832§ 2840
–	1428	1425	v ₄ NH ₄ ⁺	1426–1400* 1430† 1428–1402‡ 1430§ 1431 1475† 1460
–	1460	1457	v ₄ NH ₄ ⁺	1460

Notes: Band labels as in Figures 5b and 5c.

* Higashi (1982).

† Harlov et al. (2001).

‡ Mookherjee et al. (2002).

§ Nieto (2002).

|| Pironon et al. (2003).

Pöter et al. (2007).

ions in the interlayer site).

From inspection of the formulas in Table 7, it is apparent that there is a close chemical similarity between our samples (especially the Tob_7 crystal) and the Tobe sample (Higashi 1982), particularly in terms of the octahedral and tetrahedral sites. If the crystal from Ruiz Cruz and Sanz de Galdeano (2008) is excluded (see Fig. 6), the Tob_7 crystal is a natural tobelite with the highest ammonium content. Indeed, although the Betic Cordillera sample has higher NH₄⁺ (0.75 gpfu) concentration compared with the Tob_7 crystal, it is not, strictly speaking, a typical tobelite but is rather an intermediate dioctahedral-trioctahedral NH₄⁺-rich white mica. The NH₄⁺ content in the Tob_7 crystal is also greater than that of NH₄⁺-bearing illites and tobelites reported by Juster et al. (1987) and Nieto (2002), respectively (0.20–0.55 and 0.40–0.50 gpfu).

From a structural viewpoint, the samples studied here belong to the 2M₂ polytype, i.e., to Subfamily B polytypes (2M₂, 2O, 6H), characterized by (2n+1) × 60° rotations concerning two subsequent TOT layers (Nespolo 1999). These polytypes are not as common as Subfamily A polytypes (1M, 2M₁, 3T), which are characterized by 2n × 60° rotations (n integer). The mixed-rotation subfamily of polytypes, where both of the above mentioned rotations occur, are even more rare (Nespolo 1999). This is confirmed by the preliminary results of a HRTEM investigation of Brittany tobelite (Capitani et al. 2009) that showed that a prevalent domain of ±60° rotations of the 2M₂ stacking sequence occurs. Abundant stacking faults are associated with interruptions of these sequences; no interstratifications of 1M and 2M₂ stacking sequences are observed.

The structural features of the Musc_4 and Tob_7 crystals are compared with literature dioctahedral 2M₂ (Zhoukhlistov et al. 1973; Ni and Hughes 1996) and selected 2M₁ polytypes (Güven 1971; Rothbauer 1971; Richardson and Richardson 1982; Lin and Bailey 1984; Knurr and Bailey 1986; GA1, RA1, C3-29b samples from Brigatti et al. 1998; Westland sample from Brigatti et al. 2001a, 2001b) in Figures 7 and 8.

Figure 7 shows that the c sin(β)-cell parameter is greater in the Tob_7 than in the Musc_4 sample. Compared with other compounds, only nanpingite-2M₂ (Cs-mica) has a larger

TABLE 7. Comparison between structural formulas of the studied micas and of literature samples

	Interlayer site	Octahedral site	Tetrahedral site	Anionic site
Musc_4	(K _{0.46} Na _{0.03} Ba _{0.01} NH ₄ ⁺ _{0.36})Σ=0.86	(Al _{1.98} Mg _{0.01} Fe ³⁺ _{0.01} V ³⁺ _{0.01})Σ=2.01	(Si _{3.13} Al _{0.87})Σ=4.00	O _{10.00} F _{0.08} OH _{1.92}
Tob_7	(K _{0.18} Na _{0.01} NH ₄ ⁺ _{0.62})Σ=0.81	(Al _{1.98} Fe ³⁺ _{0.02})Σ=2.00	(Si _{3.19} Al _{0.81})Σ=4.00	O _{10.00} OH _{2.00}
Tob_Tobe*	(K _{0.19} Na _{0.01} NH ₄ ⁺ _{0.53})Σ=0.73	(Al _{1.97} Mg _{0.05} Fe ³⁺ _{0.03})Σ=2.05	(Si _{3.17} Al _{0.83})Σ=4.00	O _{10.00} OH _{2.00}
Tob_Horo*	(K _{0.27} NH ₄ ⁺ _{0.57})Σ=0.84	(Al _{1.95} Mg _{0.01} Fe ³⁺ _{0.05} Ti _{0.01})Σ=2.02	(Si _{3.09} Al _{0.91})Σ=4.00	O _{10.00} OH _{2.00}
Musc_Horo*	(K _{0.77} Na _{0.04} NH ₄ ⁺ _{0.08})Σ=0.89	(Al _{1.99} Fe ³⁺ _{0.03})Σ=2.02	(Si _{3.06} Al _{0.94})Σ=4.00	O _{10.00} OH _{2.00}
Tob†	(NH ₄ ⁺ _{1.02})Σ=1.02	(Al _{2.00})Σ=2.00	(Si _{2.98} Al _{1.02})Σ=4.00	O _{10.49}
Musc_5‡	(K _{0.39} NH ₄ ⁺ _{0.57})Σ=0.96	(Al _{2.00})Σ=2.00	(Si _{3.05} Al _{0.95})Σ=4.00	O ₁₀
Musc_6‡	(K _{0.64} NH ₄ ⁺ _{0.30})Σ=0.94	(Al _{2.00})Σ=2.00	(Si _{3.05} Al _{0.95})Σ=4.00	O ₁₀
Musc_11‡	(K _{0.81} NH ₄ ⁺ _{0.18})Σ=0.99	(Al _{2.00})Σ=2.00	(Si _{3.02} Al _{0.98})Σ=4.00	O ₁₀
Musc_12‡	(K _{0.92} NH ₄ ⁺ _{0.07})Σ=0.99	(Al _{2.00})Σ=2.00	(Si _{3.01} Al _{0.99})Σ=4.00	O ₁₀
Tob§	(K _{0.15} Na _{0.01} Ca _{0.09} NH ₄ ⁺ _{0.75})Σ=1.00	(Al _{1.70} Mg _{0.13} Fe ³⁺ _{0.26} Ti _{0.01})Σ=2.10	(Si _{2.99} Al _{1.01})Σ=4.00	O _{10.00} OH _{2.00}
Tobelitic material	(K _{0.36} Na _{0.03} NH ₄ ⁺ _{0.36})Σ=0.75	(Al _{1.91} Mg _{0.13} Fe ³⁺ _{0.03})Σ=2.07	(Si _{3.21} Al _{0.79})Σ=4.00	O _{10.00} OH _{1.88} F _{0.12}

Notes: Musc_4 and Tob_7 = crystals from this work.

Musc = ammonium muscovites; Tob = tobelites from: * Higashi (1982), † Harlov et al. (2001), ‡ Pöter et al. (2007), § Ruiz Cruz and Sanz de Galdeano (2008), and || Wilson et al. (1992).

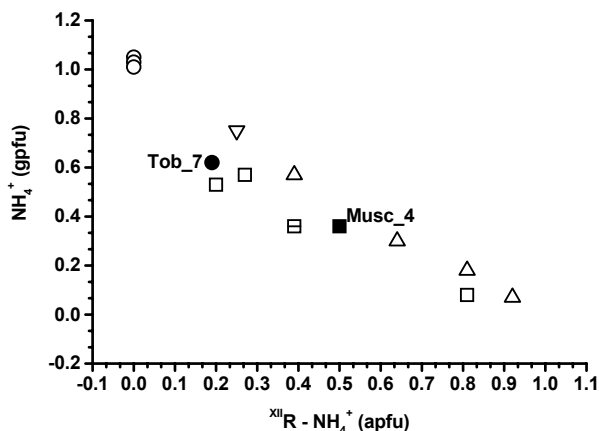


FIGURE 6. NH₄⁺ vs. ^{XII}R-NH₄⁺ diagram modified after Tischendorf et al. (2007). ^{XII}R stands for (K+Na+Ba+Ca). For comparison, all other tobelites and ammonium muscovites from literature are included. Symbols: Solid symbols = micas of this work (square: Musc_4; circle: Tob_7); open symbols = micas from literature (square: Higashi 1982; circle: Harlov et al. 2001; pointing upward triangle: Pöter et al. 2007; pointing downward triangle: Ruiz Cruz and Sanz de Galdeano 2008; square with horizontal line: Wilson et al. 1992).

interlayer site. This is essentially due to the different size of the substituting species at interlayer site [1.52 Å for ^{XII}K⁺ in muscovite (Shannon 1976), 1.69 Å for ^{XII}NH₄⁺ in tobelite (Pöter 2003), and 1.88 Å for ^{XII}Cs⁺ in nanpingite (Shannon 1976)]. However, in addition to the steric factor, other structural factors (interplay of α , Δz and the relative rotation of adjacent M layers) affect the $c \sin(\beta)$ parameter in the subfamily B polytypes (see Ferraris and Ivaldi 2002). The trigonal prismatic coordination of the interlayer cation (typical of subfamily B polytypes) is also documented in the tobelite at hand. In Figure 8, there is a slight increase of $\Delta <K-O>$ with the ditrigonal rotation angle. As expected (see Brigatti and Guggenheim 2002), the $<K-O>_{\text{inner}}$ distances, differently from the $<K-O>_{\text{outer}}$ distances, show a marked decrease as α increases. The compounds studied here show a behavior similar to muscovite, as also suggested from inspection of other distortional parameters (see Table 5).

Finally, the nature of the structural disorder in the Musc_4 and Tob_7 crystals has not been definitively clarified in the present work. It seems that two kinds of structural disorder occur. One is due to classical stacking faults, and the other is more complex and is connected with the occurrence of shifted layers as evidenced from the structure refinement of the Musc_4 crystal (see Structure determination and refinement section and Table 3) and with a shortening of the c cell parameter of ~ 1.32 Å. However, the causes of c -shortening (intergrowth/solid solutions with pyrophyllite, paragonite, phengite, etc.) cannot be unequivocally explained on the basis of X-ray diffraction considerations alone. Further insight into the nature of the stacking sequence and disorder will be addressed in a paper specifically devoted to a HRTEM investigations on Brittany tobelite crystals (in preparation).

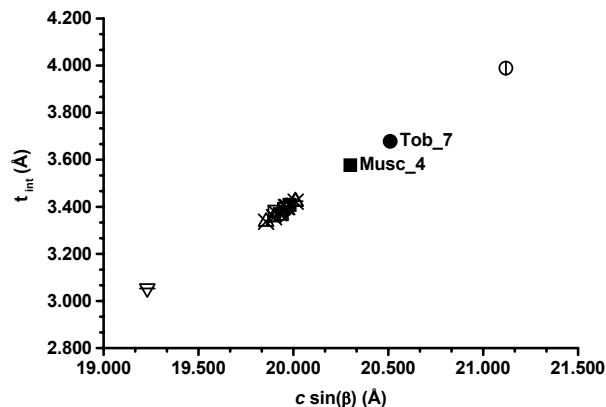


FIGURE 7. Plot of interlayer thickness (t_{int}) vs. $c \sin(\beta)$ cell parameter. For comparison, $2M_1$ and $2M_2$ dioctahedral micas from literature are included. Symbols: Solid symbols = $2M_2$ micas of this work (square: Musc_4; circle: Tob_7); open symbols with vertical line = $2M_2$ micas from literature (square: Zhoukhlistov et al. 1973; circle: Ni and Hughes 1996); open symbols with horizontal line = $2M_1$ micas from literature (square: Güven 1971; circle: Rothbauer 1971; pointing upward triangle: Richardson and Richardson 1982; pointing downward triangle: Lin and Bailey 1984; diamond: Knurr and Bailey 1986); open symbols with cross = other $2M_1$ micas from literature (square: GA1, RA1, C3-29b samples from Brigatti et al. 1998; circle: Westland sample from Brigatti et al. 2001a; pointing upward triangle: Brigatti et al. 2001b).

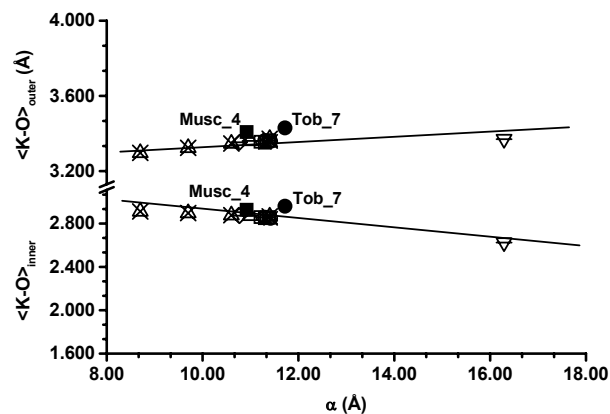


FIGURE 8. Plot of $<K-O>_{\text{inner}}$ vs. $<K-O>_{\text{outer}}$ distances vs. tetrahedral rotation angle, α . Symbols as in Figure 7. Plotted lines are guide to the eye.

ACKNOWLEDGMENTS

The authors thank J.-Louis Robert for providing the rock sample and Marcello Serracino for assistance during electron probe microanalyses at the CNR-Istituto di Geologia Ambientale e Geoingegneria (Roma). Thanks are also due to the Associate Editor, G. Henderson, who handled the paper and to M.D. Ruiz Cruz and an anonymous reviewer who helped to improve the manuscript. This work was funded by the COFIN-MIUR.

REFERENCES CITED

- Betteridge, P.W., Carruthers, J.R., Cooper, R.I., Prout, K., and Watkin, D.J. (2003) Crystals version 12: software for guided crystal structure analysis. *Journal of Applied Crystallography*, 36, 1487.
- Boyd, S.R. and Philippot, P. (1998) Precambrian ammonium biogeochemistry:

- a study of the Moine metasediments, Scotland. *Chemical Geology*, 144, 257–268.
- Brigatti, M.F. and Guggenheim, S. (2002) Mica crystal chemistry and the influence of pressure, temperature, and solid solution on atomistic models. In A. Mottana, F.P. Sassi, J.B. Thompson Jr., and S. Guggenheim, Eds., *Micas: Crystal Chemistry and Metamorphic Petrology*, 46, p. 1–97. Reviews in Mineralogy and Geochemistry, Mineralogical Society of America, Chantilly, Virginia.
- Brigatti, M.F., Frigieri, P., and Poppi, L. (1998) Crystal chemistry of Mg-, Fe-bearing muscovites-2M₁. *American Mineralogist*, 83, 775–785.
- Brigatti, M.F., Galli, E., Medici, L., Poppi, L., Cibir, G., Marcelli, A., and Mottana, A. (2001a) Chromium-containing muscovite: crystal chemistry and XANES spectroscopy. *European Journal of Mineralogy*, 13, 377–389.
- Brigatti, M.F., Kile, D.E., and Poppi, M. (2001b) Crystal structure and crystal chemistry of lithium-bearing muscovite-2M₁. *Canadian Mineralogist*, 39, 1171–1180.
- Burla, M.C., Camalli, M., Carrozzini, B., Cascarano, G.L., Giacovazzo, C., Polidori, G., and Spagna, R. (2003) SIR2002: the program. *Journal of Applied Crystallography*, 36, 1103.
- Capitani, G., Schingaro, E., and Scordari, F. (2009) HRTEM investigation of tobelite-2M₂: implication for crystal structure refinement. In *Geoitalia, Federazione Italiana di Scienze della Terra, Epitome*, 3, 14. VII Forum Italiano di Scienze della Terra, Geoitalia 2009, Rimini, Italia, ISSN 1972-1552.
- Dainyak, L.G., Drits, V.A., Zviagina, B.B., and Lindegreen, H. (2006) Cation redistribution in the octahedral sheet during diagenesis of illite-smectites from Jurassic and Cambrian oil source rock shales. *American Mineralogist*, 91, 589–603.
- Donnay, G., Morimoto, N., Takeda, H., and Donnay, J.D.H. (1964a) Trioctahedral one-layer micas. I. Crystal structure of a synthetic iron mica. *Acta Crystallographica*, 17, 1369–1373.
- Donnay, G., Donnay, J.D.H., and Takeda, H. (1964b) Trioctahedral one-layer micas. II. Prediction of the structure from composition and cell dimensions. *Acta Crystallographica*, 17, 1374–1381.
- Drits, V.A., Lindgreen, H., and Salyn, A.L. (1997) Determination of the content and distribution of fixed ammonium in illite-smectite by X-ray diffraction: Application to North Sea illite-smectite. *American Mineralogist*, 82, 79–87.
- Duit, W., Jansen, J.B.H., Van Breemen, A., and Bos, A. (1986) Ammonium micas in metamorphic rocks as exemplified by Dome de l'Agout (France). *American Journal of Science*, 286, 702–732.
- Ferraris, G. and Ivaldi, G. (2002) Structural features of micas. In A. Mottana, F.P. Sassi, J.B. Thompson Jr., and S. Guggenheim, Eds., *Micas: Crystal Chemistry and Metamorphic Petrology*, 46, p. 117–154. Reviews in Mineralogy and Geochemistry, Mineralogical Society of America, Chantilly, Virginia.
- Güven, N. (1971) The crystal structures of 2M₁ phengite and 2M₁ muscovite. *Zeitschrift für Kristallographie*, 134, 196–212.
- Harlov, D.E., Andrut, M., and Pöter, B. (2001) Characterisation of tobelite (NH₄)Al₂[AlSi₃O₁₀](OH)₂ and ND₄-tobelite (ND₄)Al₂[AlSi₃O₁₀](OD)₂ using IR spectroscopy and Rietveld refinement of XRD spectra. *Physics and Chemistry of Minerals*, 28, 268–276.
- Hazen, R.M. and Burnham, C.W. (1973) The crystal structures of one-layer phlogopite and annite. *American Mineralogist*, 58, 889–900.
- Higashi, S. (1982) Tobelite, a new ammonium dioctahedral mica. *Mineralogical Journal*, 11, 138–146.
- (2000) Ammonium-bearing mica and mica/smectite of several pottery stone and pyrophyllite deposits in Japan: their mineralogical properties and utilization. *Applied Clay Science*, 16, 171–184.
- Honna, H. and Ithara, Y. (1981) Distribution of ammonium in minerals of metamorphic and granitic rocks. *Geochimica et Cosmochimica Acta*, 45, 983–988.
- Hovis, G.L., Harlov, D., and Gottschalk, M. (2004) Solution calorimetric determination of the enthalpies of formation of NH₄-bearing minerals buddingtonite and tobelite. *American Mineralogist*, 89, 85–93.
- Ithara, Y. and Suwa, K. (1985) Ammonium contents of biotites from Precambrian rocks in Finland: The significance of NH₄⁺ as a possible chemical fossil. *Geochimica et Cosmochimica Acta*, 49, 145–151.
- Juster, T.C., Brown, P.E., and Bailey, S.W. (1987) NH₄-bearing illite in very low grade metamorphic rocks associated with coal, northeastern Pennsylvania. *American Mineralogist*, 72, 555–565.
- Knurr, R.A. and Bailey, S.W. (1986) Refinement of Mn-substituted muscovite and phlogopite. *Clays and Clay Minerals*, 34, 7–16.
- Liang, S., Ren, D., Wang, S., and Yao, G. (1997) Study of aluminum hydroxide minerals in tonsteins from Carboniferous-Permian coal-bearing series in Northern China. *Chinese Journal of Geology (Scientia Geologica Sinica)*, 32, 478–486.
- Lin, C.Y. and Bailey, S.W. (1984) The crystal structure of paragonite-2M₁. *American Mineralogist*, 69, 122–127.
- Mingram, B. and Bräuer, K. (2001) Ammonium concentration and nitrogen isotope composition in metasedimentary rocks from different tectonometamorphic units of the European Variscan Belt. *Geochimica et Cosmochimica Acta*, 65, 273–287.
- Mookherjee, M., Redfern, S.A.T., Zhang, M., and Harlov, D.E. (2002) Orientational order-disorder of N(D,H)₄⁺ in tobelite. *American Mineralogist*, 87, 1686–1691.
- Nespolo, M. (1999) Analysis of family reflections of OD mica polytypes, and its application to twin identification. *Mineralogical Journal*, 21, 53–85.
- Ni, Y. and Hughes, J.M. (1996) The crystal structure of nanpingite-2M₂, the Cs end-member of muscovite. *American Mineralogist*, 81, 105–110.
- Nieto, F. (2002) Characterization of coexisting NH₄⁺ and K-micas in very low-grade metapelites. *American Mineralogist*, 87, 205–216.
- Pironon, J., Pelletier, M., de Donato, P., and Mosser-Ruck, R. (2003) Characterization of smectite and illite by FTIR spectroscopy of interlayer NH₄⁺ cations. *Clay Minerals*, 38, 201–211.
- Pöter, B. (2003) Experimentally determined K-NH₄ partitioning between feldspars, muscovites and aqueous chloride solutions, 102 p. Ph.D. thesis, University of Berlin, Germany.
- Pöter, B., Gottschalk, M., and Heinrich, W. (2007) Crystal-chemistry of synthetic K-feldspar-buddingtonite and muscovite-tobelite solid solutions. *American Mineralogist*, 92, 151–165.
- Pouchou, J.L. and Pichoir, F. (1985) "PAP" $\Phi(\rho Z)$ procedure for improved quantitative microanalysis. In J.T. Armstrong, Ed., *Microbeam Analysis*, p. 104–106. San Francisco Press, California.
- Richardson, S.M. and Richardson, J.W. (1982) Crystal structure of a pink muscovite from Archer's Post, Kenya: implications for reverse pleochroism in dioctahedral micas. *American Mineralogist*, 67, 69–75.
- Rieder, M., Cavazzini, G., D'Yakonov, Y.S., Frank-Kamenetskii, V.A., Gottardi, G., Guggenheim, S., Koval', P.V., Müller, G., Neiva, A.M.R., Radoslovich, E.W., Robert, J.-L., and others. (1998) Nomenclature of the micas. *Canadian Mineralogist*, 36, 41–48.
- Rothbauer, V.R. (1971) Untersuchung eines 2M₁-Muskovits mit Neutronenstrahlen. *Neues Jahrbuch für Mineralogie, Monatshefte*, 143–154.
- Ruiz Cruz, M.D. (2011) NH₄-bearing micas in poly-metamorphic Alpujarride micaschists and gneisses from the central zone of the Betic Cordillera (Spain): tectono-metamorphic and crystal-chemical constraints. *Mineralogy and Petrology*, 101, 225–244.
- Ruiz Cruz, M.D. and Sanz de Galdeano, C. (2008) High-temperature ammonium white mica from the Betic Cordillera (Spain). *American Mineralogist*, 93, 977–987.
- (2009) Suhailite, a new ammonium trioctahedral mica. *American Mineralogist*, 94, 210–221.
- (2010) Factors controlling the evolution of mineral assemblages and illite crystallinity in Paleozoic to Triassic sequences from the transition between Maláguide and Alpujarride complexes (Betic Cordillera, Spain): the significance of tobelite. *Clays and Clay Minerals*, 58, 570–584.
- Schroeder, P.A. and Ingall, E.D. (1994) A method for the determination of nitrogen in clays, with application to the burial diagenesis of shales. *Journal Sedimentary Research A*, 64, 694–697.
- Schroeder, P.A. and McLain, A.A. (1998) Illite-smectite and the influence of burial diagenesis on the geochemical cycling of nitrogen. *Clay Minerals*, 33, 539–546.
- Shannon, R.D. (1976) Revised effective ionic radii and systematic studies of interatomic distances in halides and chalcogenides. *Acta Crystallographica*, A32, 751–767.
- Sheldrick, G.M. (2004) SADABS. University of Göttingen, Germany.
- Siemens (2004) SMART, SAINT (version 7.23A). Siemens Analytical X-ray Instruments, Madison, Wisconsin.
- Tischendorf, G., Förster, H.-J., Gottesmann, B., and Rieder, M. (2007) True and brittle micas: composition and solid-solution series. *Mineralogical Magazine*, 71, 285–320.
- Toraya, H. (1981) Distortions of octahedra and octahedral sheets in 1M micas and the relation to their stability. *Zeitschrift für Kristallographie*, 157, 173–190.
- Visser, D. (1992) On ammonium in upper-amphibolite facies cordierite-ortho-amphibole-bearing rocks from Rod, Bamble Sector, south Norway. *Norsk Geologisk Tidsskrift*, 72, 385–388.
- Wilson, P.N., Parry, W.T., and Nash, W.P. (1992) Characterization of hydrothermal tobelitic veins from black shale, Quirrh Mountains, Utah. *Clays and Clay Minerals*, 40, 405–420.
- Zhoukhlistov, A.P., Zvyagin, B.B., Soboleva, S.V., and Fedotov, A.F. (1973) The crystal structure of the dioctahedral mica 2M₂ determined by high voltage electron diffraction. *Clays and Clay Minerals*, 21, 465–470.